

Precision spectrophotometry for PNLF distances: the case of NGC 300

Azlizan A. Soemitro^{1,2}, Martin M. Roth^{1,2}, Peter M. Weilbacher¹, Robin Ciardullo³, George H. Jacoby⁴, Ana Monreal-Ibero⁵, Norberto Castro¹, Genoveva Micheva¹

¹Leibniz-Institut für Astrophysik Potsdam (AIP), Germany

²Universität Potsdam, Germany

³Department of Astronomy & Astrophysics, The Pennsylvania State University, USA

⁴NSF's NOIRLab, Tucson, USA

⁵Leiden Observatory, Leiden University, The Netherlands

Abstract. The Multi-Unit Spectroscopic Explorer (MUSE) has enabled a renaissance of the planetary nebula luminosity function (PNLF) as a standard candle. In the case of NGC 300, we learned that the precise spectrophotometry of MUSE was crucial to obtain an accurate PNLF distance. We present the advantage of the integral field spectrograph compared to the slit spectrograph in delivering precise spectrophotometry by simulating a slit observation on integral field spectroscopy data. We also discuss the possible systematic shift in measuring the PNLF distance using the least-square method, especially when the PNLF cutoff is affected by small number statistics.

Keywords. galaxies: luminosity function, stars: planetary nebulae

1. Introduction

The planetary nebula luminosity function (PNLF) is a secondary distance indicator with $\sim 10\%$ accuracy (Ciardullo 2010, 2022). Using narrowband photometry, one can obtain the V-band equivalent [OIII] $\lambda 5007$ magnitude defined by Jacoby (1989):

$$m_{5007} = -2.5 \log F_{5007} - 13.74 \quad (1)$$

The number distribution of planetary nebulae (PNe) per magnitude bin for a given galaxy can then be modelled using the empirical law described by Ciardullo et al. (1989):

$$N(M) \propto e^{0.307M} \{1 - e^{3(M^* - M)}\} \quad (2)$$

Variations of the formula have been introduced to explain the influence of different underlying stellar populations (Longobardi et al. 2013; Rodríguez-González et al. 2015). However, these formulae merely affect the faint end of the PNLF. The definition of the PNLF cutoff, which is crucial for the distance determination, remains unchanged.

The renaissance of the PNLF as standard candles came with the use of the Multi-Unit Spectroscopic Explorer (MUSE; Bacon et al. 2010) on the Very Large Telescope (VLT). As an integral field spectrograph (IFS), it allows simultaneous imaging and spectroscopy to find and classify PNe, even in more crowded regions of galaxies, that previously were not accessible using the classical narrow-band imaging methods (Kreckel et al. 2017; Spriggs et al. 2020; Roth et al. 2021; Scheuermann et al. 2022; Soemitro et al. 2023).

The precision of the m_{5007} defines the precision of the PNLF cutoff of a galaxy, which consequently defines the accuracy of the distance determination. To achieve this, Roth et al. (2021) developed the differential emission line filter (DELFI), which suppresses systematic

errors and delivers higher signal-to-noise ratios for the photometry, with a typical photometric error of ~ 0.04 mag. They demonstrated that their method was able to reach distances up to ~ 40 Mpc, twice as far as most studies done with the classical narrow-band photometry until the early 2010s.

2. Planetary nebulae in NGC 300

NGC 300 is a nearby spiral galaxy in the foreground of the Sculptor Group, where a few PN surveys have already been conducted, making it a good case to test the DELF technique using MUSE data (Soemitro et al. 2023). Previously, using narrow-band imaging on the New Technology Telescope (NTT), Soffner et al. (1996) found 34 PNe, covering $3 \times 2.2 \times 2.2$ arcmin². Another survey with the FORS2 instrument on the VLT found a total of 104 PNe using the narrow-band imaging mode within $2 \times 6.8 \times 6.8$ arcmin² (Peña et al. 2012). For the brighter 32 PN candidates, they obtained spectroscopic follow-up data using the multi object spectroscopy mode of the same instrument (MXU-FORS2). Using the MUSE instrument, Roth et al. (2018) observed 7 fields in the wide field mode (WFM, 1×1 arcmin² FoV) that cover the nucleus, parts of a spiral arm, and parts of a nearby inter-arm region, as a pilot study for crowded field spectroscopy, which explored a plethora of possible science cases. They identified 45 PNe, which was not ideal to construct a proper PNLF. As a follow up for the PN science case, Soemitro et al. (2023) employed additional archival MUSE data and increased the dataset from 7 fields to a total of 44 fields, and identified 109 PNe. Using the DELF, the study presented a similar number of PNe in comparison to the previous study by Peña et al. (2012), however needing only half of the surveyed area.

3. Precision spectrophotometry: integral field spectrograph vs. slit spectrograph

For the common PNe in the sample, Soemitro et al. (2023) have compared the m_{5007} measurements with the results from Soffner et al. (1996) and Peña et al. (2012). While their m_{5007} values were consistent with the earlier study done with the narrow-band imaging photometry on the NTT, they found that the results from the FORS2 survey study were fainter by an average of 0.71 mag, a discrepancy factor of ~ 2 . The m_{5007} comparison can be seen in Figure 1. The speculation was, since Peña et al. (2012) calibrated their photometry using spectroscopic fluxes obtained with the multi object spectrograph, that they might be subject to slit loss effects (Soemitro et al. 2023). Due to atmospheric dispersion, one has to orient the slit along the parallactic angle to obtain precise spectrophotometry (Filippenko 1982; Jacoby & Kaler 1993). This is necessary to minimise the slit loss, because the wavelength dependence of the point spread function full width half maximum (PSF FWHM) might complicate the slit positioning. For instance, if the slit was positioned based on the image in the R-band, the slit position could be off-centre at [OIII] λ 5007. Moreover, the PSF FWHM also increases with shorter wavelengths (Fried 1966; Boyd 1978; Kamann et al. 2013), which might causes more loss of flux in blue.

To demonstrate the effect of atmospheric dispersion, we used a standard star observation obtained with another integral field spectrograph, the Potsdam Multi-Aperture Spectrophotometer (PMAS; Roth et al. 2005) whose raw data comes without atmospheric dispersion correction. The star was observed in the lens array mode with $1''/\text{pixel}$ sampling (LARR, 16×16 arcmin² FoV) and a wavelength coverage of $\sim 3500 - 6800$ Å (V600 Grating, GROT=144.5). We took two wavelength slices: 3800 Å and 6500 Å. We created a rectangular aperture to simulate a slit, using the width of two pixels. The simulated slit position was fixed based on the PSF centroid in 6500 Å, then we performed photometry for both slices. As a comparison, we also did photometry using circular apertures with the radius of two pixels, however, we adjusted their positions based on the PSF centroid in each respective data cube layer. Figure 2 displays the star with the apertures in the two wavelengths. In this

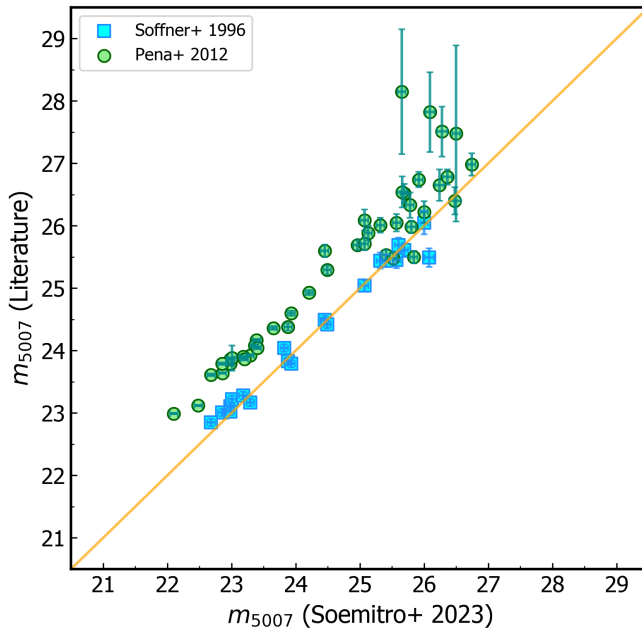


Figure 1. Comparison of the m_{5007} for different PN surveys in NGC 300. The magnitudes from Peña et al. (2012) is 0.71 mag fainter than the other surveys. The plot is adapted from Soemitro et al. (2023).

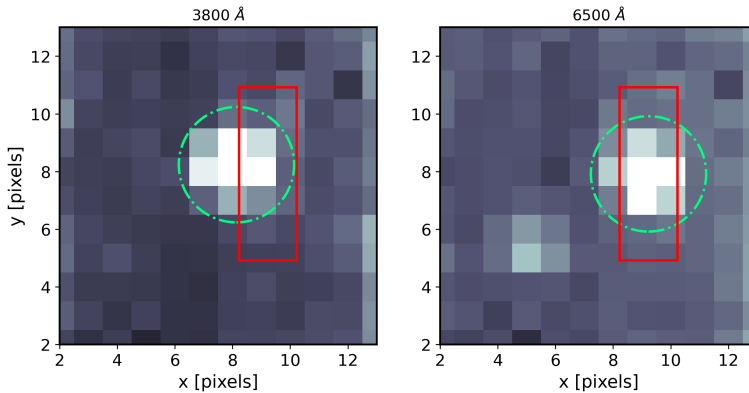


Figure 2. Simulated apertures for testing the light loss effect of atmospheric dispersion for a standard star. The dot-dashed green line represents measurements using IFS. The solid red line represent measurements using a slit spectrograph. This effect can be minimised by aligning the slit with the parallactic angle continuously during observations (Filippenko 1982; Jacoby & Kaler 1993).

configuration, we found that the slit loss in 6500 Å was $\sim 10\%$. However, with $\sim 34\%$, the light loss in the blue was much more severe.

While we cannot prove that the effect was exactly the cause of the discrepancies between Peña et al. (2012) and Soemitro et al. (2023), since it was unclear whether the slit alignment with the parallactic angle was done or not for the FORS2 observations, we can plausibly argue that the effect can have large effects on the flux calibration, in particular knowing that the seeing FWHM can be quite variable over the course of a night. Moreover, we demonstrated that the IFS has an advantage to handle such atmospheric effects, delivering a more precise spectrophotometry and consequently better distances. In the case of MUSE data, the

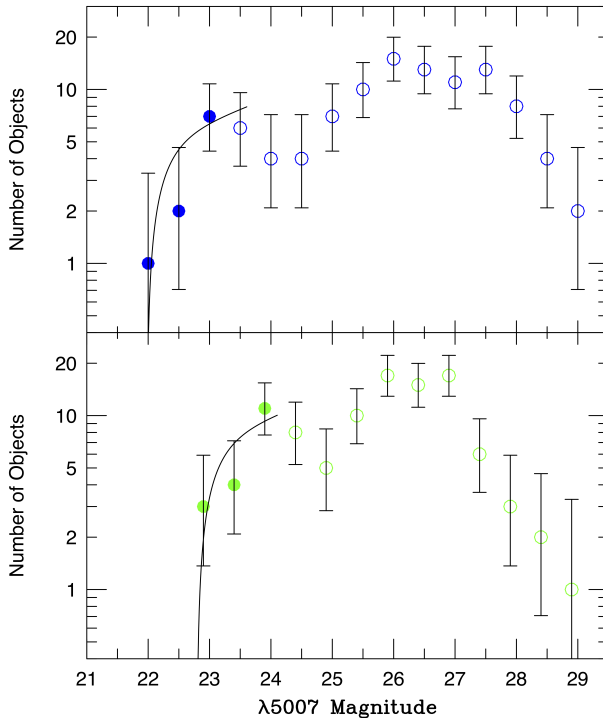


Figure 3. The PNLF for MUSE data (Soemitro et al. 2023) in blue and FORS2 data (Peña et al. 2012) in green. The plot is adapted from Soemitro et al. (2023).

atmospheric dispersion as a function of wavelength is even corrected by lateral shifts that are applied through the data reduction pipeline (Weilbacher et al. 2020).

4. The PNLF of NGC 300

In Soemitro et al. (2023), the PNLF distance to NGC 300 was derived using the maximum likelihood estimation method (Ciardullo et al. 1989). The PNLF maximum likelihood distance estimates for both the MUSE and the FORS2 datasets resulted in $(m - M)_0 = 26.48^{+0.11}_{-0.26}$ and $(m - M)_0 = 27.30^{+0.09}_{-0.20}$, respectively, reflecting the photometric discrepancy explained above. However, in the original study of Peña et al. (2012), they measured a distance of $(m - M)_0 = 26.29^{+0.12}_{-0.22}$, derived on the basis of the least-square fitting method. By using such a method, the distance measurement became very dependent on the binning. Since the PNLF bins of NGC 300 presented only a small number of PNe, the exact definition of the bins has likely caused a systematic shift to the distance measurement (Soemitro et al. 2023). The choice of binning also smeared out the details of the PNLF shape. In their study, Peña et al. (2012) reported that they did not observe any PNLF dip, that however is typically being observed in star forming galaxies (Jacoby & De Marco 2002). With a higher resolution of the magnitude bins, Soemitro et al. (2023) showed that the dip can be seen even in the FORS2 data, and also in the MUSE observations, as shown in Figure 3. With the precise spectrophotometry delivered by MUSE, the PNLF distance was brought into good agreement with the Cepheid and the tip of the red giant branch (TRGB) distances. The distance comparison is shown in Figure 4.

5. Summary

The case of NGC 300 has shown that the precision of spectrophotometry can have a significant impact on the distance measurement. We made a test using another integral field

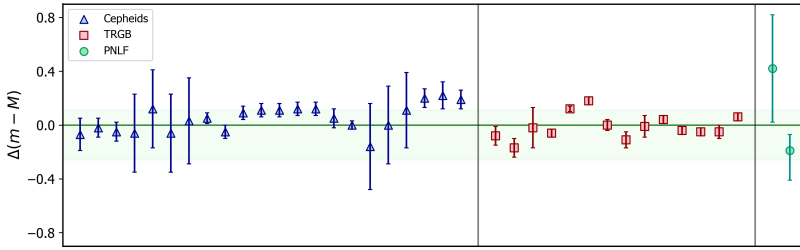


Figure 4. The MUSE-PNLF distance and its uncertainty is presented as a solid green line and the green shaded range, respectively. As a comparison with distances from literature, Cepheids (blue triangles), tip of the red giant branch (red squares), and previous PNLF distance estimates (the two green circles) are shown. A full reference list of literature distances can be found in [Soemitro et al. \(2023\)](#).

spectrograph, PMAS, to show the probable effect of atmospheric dispersion when using a slit spectrograph to do the spectrophotometry. This illustration supports the importance of using an IFS for measuring accurate m_{5007} magnitudes for PNLF distance determinations. Moreover, the methodology of how to fit an analytical PNLF to the observed photometry is crucial. In case of small number statistics at the PNLF cutoff, using the least-square minimisation method that is dependent on the bin size, is likely to bias the distance measurement. Therefore, the maximum likelihood approach is recommended. As the only IFS that to date has the sensitivity and spatial resolution to detect PNe in distant galaxies, the MUSE instrument is crucial for the measurement of PNLF distances in the future. With the currently demonstrated range of up to ~ 40 Mpc, the PNLF can be assumed to be an additional calibration tool for SN Ia distances and a contribution to the ongoing discussion of the Hubble tension ([Jacoby et al. 2023](#)).

References

- Bacon, R. et al. 2010, SPIE, 7735, 773508
 Boyd, J. P. 1978, Journal of Atmospheric Sciences, 35, 2236
 Ciardullo, R. 2010, PASA, 27, 149
 Ciardullo, R. 2022, Frontiers in Astronomy and Space Sciences, 9, 896326
 Ciardullo, R. et al. 1989, ApJ, 339, 53
 Filippenko, A. V. 1982, PASP, 94, 715
 Fried, D. L. 1966, Journal of the Optical Society of America (1917-1983), 56, 1372
 Jacoby, G. H. 1989, ApJ, 339, 39
 Jacoby, G. H., Ciardullo, R., Roth, M. M., Arnaboldi, M., & Weillbacher, P. M. 2023, arXiv e-prints, arXiv:2309.11603
 Jacoby, G. H. & De Marco, O. 2002, AJ, 123, 269
 Jacoby, G. H. & Kaler, J. B. 1993, ApJ, 417, 209
 Kamann, S., Wisotzki, L., & Roth, M. M. 2013, A&A, 549, A71
 Kreckel, K. et al. 2017, ApJ, 834, 174
 Longobardi, A. et al. 2013, A&A, 558, A42
 Peña, M. et al. 2012, A&A, 547, A78
 Rodríguez-González, A. et al. 2015, A&A, 575, A1
 Roth, M. M. et al. 2005, PASP, 117, 620
 Roth, M. M. et al. 2018, A&A, 618, A3
 Roth, M. M. et al. 2021, ApJ, 916, 21
 Scheuermann, F. et al. 2022, MNRAS, 511, 6087
 Soemitro, A. A. et al. 2023, A&A, 671, A142
 Soffner, T. et al. 1996, A&A, 306, 9
 Spriggs, T. W. et al. 2020, A&A, 637, A62
 Weillbacher, P. M. et al. 2020, A&A, 641, A28